ChemComm

First principles Monte Carlo simulations of unary and binary adsorption: CO2, N2, and H2O in Mg-MOF-74

Journal:	*ChemComm*
Manuscript ID	CC-COM-07-2018-006178.R1
Article Type:	Communication

Journal Name

ARTICLE TYPE

Cite this: DOI: 10.1039/xxxxxxxxxx

First principles Monte Carlo simulations of unary and binary adsorption: CO_2, N_2, and H_2O in Mg-MOF-74†

Evgenii O. Fetisov,[a] Mansi S. Shah,[ab], Jeffrey R. Long,[cd] Michael Tsapatsis,[b] and J. Ilja Siepmann*[ab]

Received Date
Accepted Date

DOI: 10.1039/xxxxxxxxxx

www.rsc.org/journalname

Dative bonding of adsorbate molecules onto coordinatively-unsaturated metal sites in metal–organic frameworks (MOFs) can lead to unique adsorption selectivities. However, the significant distortion of the electron density during dative bonding poses a challenge for force-field-based simulations. Here, we report first principles Monte Carlo simulations with the PBE-D3 functional for the adsorption of CO_2, N_2, and H_2O in Mg-MOF-74, and obtain accurate predictions of the unary isotherms without any of the adjustments or fitting often required for systems with strong adsorption sites. Simulations of binary CO_2/N_2 and H_2O/CO_2 mixtures yield selectivities of 200 and 160, respectively, and indicate that predictions from ideal adsorbed solution theory need to be viewed with caution.

In recent years, metal–organic frameworks (MOFs) have emerged as promising nanoporous materials of choice for many industrially relevant processes and environmental applications.[1] One of the most active areas of research remains exploration of MOFs for adsorption-based processes. Highly tunable framework properties (e.g., surface area and chemical functionalization) allow for MOFs to be tailored toward specific tasks, including methane storage,[2] carbon capture,[3] and sour gas sweetening.[4] Additionally, diverse libraries of chemical building blocks can be used to computationally construct large databases of MOFs or to utilize evolutionary strategies for high-throughput screening studies.[5,6]

Here, we focus on CO_2 capture in Mg_2(dobdc) (dobdc^{4-} = 2,5-dioxido-1,4-benzenedicarboxylate), also known as Mg-MOF-74 or CPO-27-Mg, from flue gas – a process extensively studied both experimentally and computationally.[7] Due to the high density of open metal sites in MOF-74 (18 per unit cell) and their strong and selective dative bonding with adsorbates possessing lone-pair electrons (via formation of a 2-center, 2-electron bond and the associated charge transfer from the adsorbate to the metal node), special computational approaches need to be applied to accurately describe these adsorbate–adsorbent systems. Two approaches are commonly used to overcome limitations of generalized molecular-mechanics force fields (GMMFFs). In the first one, specific guest–host force field parameters are determined using quantum-mechanical calculations for clusters or periodic structures and subsequently used in conventional Monte Carlo (MC) simulations to probe adsorption isotherms.[8–11] In the second one, *ab initio* free energies of adsorption of a single molecule bonding to specific sites are obtained and multi-site Langmuir models are used to generate adsorption isotherms.[12] Both approaches have their own limitations and, most importantly, do not account for the change in adsorbate–adsorbate interactions caused by one or both of them being involved in a dative bond, but ultimately they perform much better than GMMFFs for these systems.

The authors of the pioneering study utilizing quantum-mechanically derived force fields (QMDFFs) stated that quantum chemical calculations of the energy of each configuration along the simulation trajectory would be ideal but at the same time would be prohibitively expensive.[8] Advances in periodic density functional theory (DFT) methods[18] and MC sampling algorithms combined with the steady increase in available computational power now allow for such first principles Monte Carlo (FPMC) simulations of adsorption systems to be a realistic goal.

Use of FPMC for the simulation of phase equilibria is not a novel concept and goes back to as early as 2006, when it was first applied to study vapor–liquid equilibria (VLE) of water.[19] Here, we

[a] *Department of Chemistry and Chemical Theory Center, University of Minnesota, 207 Pleasant Street SE, Minneapolis, Minnesota 55455, USA.*
[b] *Department of Chemical Engineering and Materials Science, University of Minnesota, 421 Washington Avenue SE, Minneapolis, Minnesota 55455, USA.*
[c] *Department of Chemistry and Chemical & Biomolecular Engineering, University of California, Berkeley, Berkeley, California 94720-1462, USA.*
[d] *Materials Sciences Division, Lawrence Berkeley National Laboratory, Berkeley, California 94720, USA.*
* *Corresponding Author E-mail: siepmann@umn.edu*
† Electronic Supplementary Information (ESI) available: Computational and analysis details, numerical results. See DOI: 10.1039/b000000x/

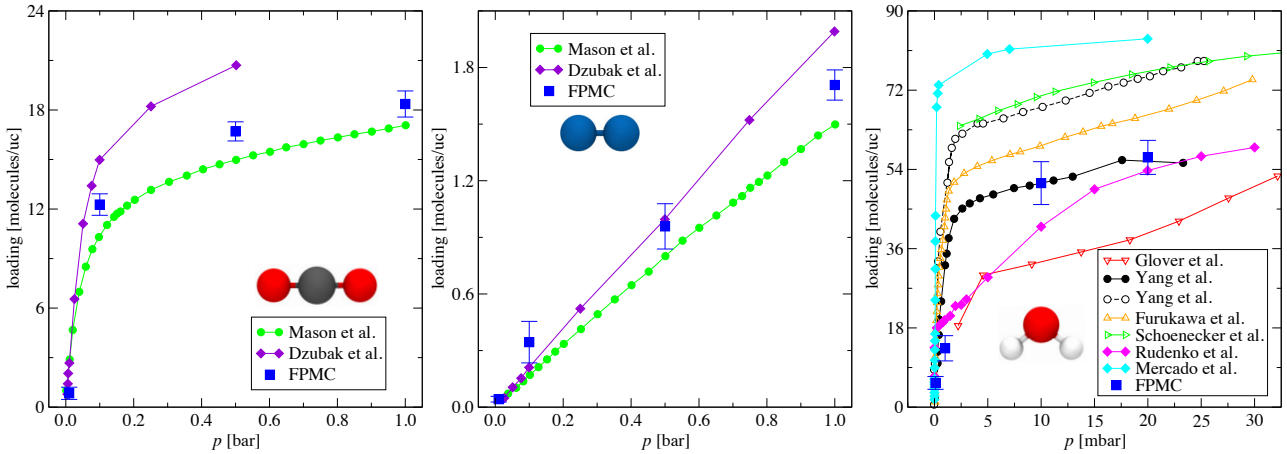

Fig. 1 Unary adsorption isotherms for CO_2 (left), N_2 (middle), and H_2O (right) in Mg-MOF-74 measured experimentally (Mason *et al.*[13], Glover *et al.*[14], Yang *et al.*[15], Schoenecker *et al.*[16], Furukawa *et al.*[17]), predicted using QMDFFs (Dzubak *et al.*[8], Rudenko *et al.*[9], Mercado *et al.*[11]), and using FPMC (where the error bars represent standard errors of the mean from 16 independent simulations). Note the differences in the axis scales.

retain the FPMC framework, but apply it to probe the adsorption of CO_2, N_2, and H_2O in Mg-MOF-74. These three molecules have the capability to participate in dative bonding. In addition to capturing the changes in the electronic structure associated with dative bonds, use of DFT for the energy calculations of the entire periodic system also enables one to treat structural distortions of adsorbate and adsorbent.

As also for VLE, the FPMC simulations for adsorption are carried out in the Gibbs ensemble using two or more periodic simulation boxes,[20] but here the low-density gas-phase reservoir is treated as an ideal gas and neither the volume nor shape of the adsorbent box is allowed to change. The former approximation allows us to compute the configurational energy of the reservoir containing flexible molecules as the sum of the energies of isolated molecules, each computed for a box with similar volume (and, hence, grid spacing for the plane wave computation) as the adsorbent box, i.e., avoiding DFT calculations for computationally unaffordably large volumes of the entire reservoir. Similarly, retaining volume and shape of the adsorbent box reduces computational expense by allowing a smaller charge density cut-off for the DFT calculations,[21] and it is justified by experimental data for the Mg-MOF-74 system.[22] When adsorption leads to large-scale changes of the adsorbent structure,[23–25] then the constant-stress version of the Gibbs ensemble should be employed.[26]

The configurational space is sampled here through various MC moves: molecule transfers between the vapor and adsorbent phases, translations and rotations of adsorbate molecules only in the adsorbent phase, atom displacements to sample adsorbate conformation (in both phases) and local changes of the adsorbent structure, hybrid molecular dynamics/MC moves[27] to sample collective rearrangements of the guest–host system, volume displacements for the total volume of the ideal-gas reservoir. In order to avoid highly unfavorable trial configurations (where DFT calculations would not converge) and to reduce the frequency of DFT calculations, configurational-bias MC techniques for molecule transfers and pre-sampling using an inexpensive approximate potential are employed.[19,28,29]

Utilizing the FPMC approach with the widely used and robust PBE-D3[30,31] density functional, we compute the unary adsorption isotherms for CO_2, N_2, and H_2O in Mg-MOF-74 at $T = 313$ K and four pressures for each compound (note that all atoms are in a closed-shell electronic configuration). Isotherms from experimental measurements,[13–15] from simulations with QMDFFs,[8,9,11] and from the present FPMC simulations are compared in Fig. 1. The FPMC results more accurately follow the experimental loading for CO_2 and N_2 measured by Mason *et al.*[13] compared to the predictions by Dzubak *et al.*[8] using a force field derived from MP2 calculations. At $p = 1$ bar, the FPMC simulations yield a CO_2 loading of just above 18, i.e., one adsorbate per open metal site. For H_2O, there is a significant spread of the experimental data due to water's stronger binding affinity and higher loading,[13–17] but the FPMC predictions fall within the experimental range and exhibit a type I isotherm shape with a saturation loading exceeding the number of open metal sites by a factor of 3. It should be noted, however, that experimental data for water were obtained at ~ 300 K, whereas our simulations are performed at 313 K; an increase in temperature would shift the experimental isotherms to slightly higher pressures.

Previously, Peng *et al.*[32] surmised that all GMMFFs fail to predict correct trends for H_2O loading and empirical adjustments are required in order to get reasonable agreement. Moreover, the isotherm computed by Rudenko *et al.*[9] with a QMDFF exhibits a kink as the loading exceeds 18 molecules that could attributed to inadequate description of adsorbate–adsorbate interactions due to different force fields. This again showcases the strength of FPMC that incorporates changes in the adsorbate–adsorbate interactions when dative bonding causes changes in the electronic structure of the adsorbed molecule. Overall, these results indicate that the FPMC approach is indeed promising as a fully predictive method, although the final results will ultimately depend on the choice of the underlying level of theory (density functional), especially, for adsorbents exhibiting chemisorption.[33]

One of the advantages of the FPMC approach when applied to adsorption is that thermally-averaged adsorption enthalpies for

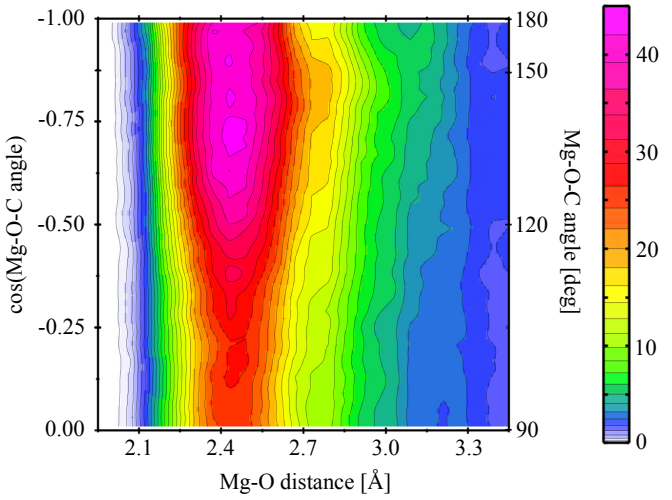

Fig. 2 Radial–angular distribution between CO_2 and Mg in Mg-MOF-74 at $T = 313$ K and $p_{CO_2} = 1$ bar. A value of unity on the color scale corresponds to a uniform distribution over distances and angles.

the different state points are readily available from the simulation trajectories. In contrast, adsorption energies are commonly computed via static quantum-chemical calculations involving a single adsorbate molecule and thermal motion is only accounted for through the harmonic approximation. FPMC trajectories include anharmonic effects, confinement effects, and adsorbate–adsorbate interactions. However, it should be noted that the current FPMC simulations sample from the classical partition function and therefore do not account for nuclear quantum effects that should be small for the present systems due to the relatively high adsorbate molecular weight and the high temperature. From our unary simulations, we find that the adsorption enthalpies of CO_2 and N_2 remain constant (within the statistical uncertainties) for the loadings observed here that do not exceed the number of open metal sites. The calculated values of 42 ± 7 kJ/mol for CO_2 and 26 ± 4 kJ/mol for N_2 agree well with the experimental data [13,22,34,35] of 43–48 and 21–25 kJ/mol, respectively. For H_2O, we obtain values of 68 ± 5 and 61 ± 4 kJ/mol for the state points with loadings below and above, respectively, the number of open metal sites; these values are somewhat smaller than the 73–80 kJ/mol range reported by Tan *et al.* [35]

The FPMC trajectories also yield structural information at the actual adsorption conditions. For the adsorption of CO_2, geometry optimization with various electronic structure methods yields a Mg–O distance of 2.31–2.37 Å, a Mg–O–C angle of 129–136°, and an O–C–O angle of 177–178°. [8,34] Experimental data measured at $T = 10$ K yields a Mg–O distance of 2.27 ± 0.01 Å, a Mg–O–C angle of $(131 \pm 1)°$, and an O–C–O angle of $(178 \pm 2)°$ in agreement with static electronic structure results. [22] Fig. 2 shows the radial–angular distribution for the binding of CO_2 to the open metal site obtained at $p = 1$ bar (i.e., a loading of about 1 CO_2 molecule per metal). Thermal motion leads to an increase of the Mg–O distance to 2.45 ± 0.10 Å. Even more pronounced is the angular broadening with angles between 120 and 180° being most preferred, but the relative probability to observe a 90° angle is only smaller by a factor of 2. The FPMC simulations yield an average angle of $(152 \pm 13)°$, i.e., considerably larger than the value from geometry optimizations. The thermally averaged O–C–O angle for the adsorbed CO_2 molecules is found to be $(174 \pm 2)°$ in agreement with calculations for CO_2 in the solid and supercritical phases, [36] and lower than that of the optimized geometry because entropic effects disfavor an angle of 180°.

Table 1 Loadings and computed selectivities for the CO_2/N_2 and CO_2/H_2O mixtures

	CO_2/N_2		CO_2/H_2O	
	q (FPMC) [molec/uc]	q (IAST) [molec/uc]	q (FPMC) [molec/uc]	q (IAST) [molec/uc]
CO_2	12.5 ± 0.5	13.1 ± 0.3	9.5 ± 0.8	10.1 ± 0.5
N_2 or H_2O	0.38 ± 0.09	0.07 ± 0.02	10.3 ± 1.0	9.0 ± 0.6
S_{CO_2} or S_{H_2O}	200 ± 50	1000 ± 300	160 ± 30	140 ± 20

Probing mixture adsorption is of utmost importance in the design of separation processes, e.g. CO_2 capture from flue gas, but experimental measurements are challenging and often not available. [37] Thus, the common method in determinig binary isotherms is based on the ideal adsorbed solution theory (IAST), [38] which itself relies on the knowledge of unary isotherms. However, it is not always clear when IAST is applicable and Joos *et al.* [39] have surmised that IAST usually fails for systems with strong preferential adsorption at specific sites – a condition applicable to Mg-MOF-74. The FPMC methodology can also be applied directly to investigate adsorption of gas mixtures and, hence, can serve as a test for the accuracy of IAST for this important system. We compute the loadings for a 15:85 CO_2/N_2 mixture using two ideal-gas reservoirs with a total pressure of 1 bar at 313 K, i.e., typical conditions for flue gas separation. Results obtained from the direct FPMC simulation and determined using IAST (with the unary isotherms from the FPMC simulations as input) are given in Table 1. The FPMC simulations support the very high selectivity for CO_2 also observed in breakthrough experiments. [13] The IAST-based selectivity toward CO_2 is overestimated by a factor of 5 ± 2 when compared to the direct simulation results. In comparison, Dzubak *et al.* [8] observed an overprediction of less than a factor of 2 using QMDFFs for the adsorbate–Mg interactions, but generalized force fields for the adsorbate–adsorbate interactions. The loading data (see Table 1) indicate that an underestimation of the N_2 loading predicted by IAST by a factor of 5 is the origin for the overestimation of the selectivity. Evidently, the adsorption of about 13 CO_2 molecules leads to an effective reduction of the pore diameter and a more favorable environment for N_2 than found in the bare Mg-MOF-74 pore that is not captured by IAST. The distribution of CO_2 molecules per unit cell is not significantly affected by the coadsorption of a single N_2 molecule (see Fig. 3), i.e., N_2 does not displace CO_2 from the strong adsorption sites.

Recently, it was shown that the presence of water at concentrations as low as 0.1% in a flue stream can have a detrimental influence on CO_2 loading and performance during swing adsorption processes. [40,41] The unary isotherms (see Fig. 1) indicate that H_2O adsorbs in Mg-MOF-74 even more strongly than CO_2, and its experimental detection is challenging, especially at low concentrations. Thus, we investigate the influence of water acting as an impurity on the CO_2 adsorption through FPMC simulations for the

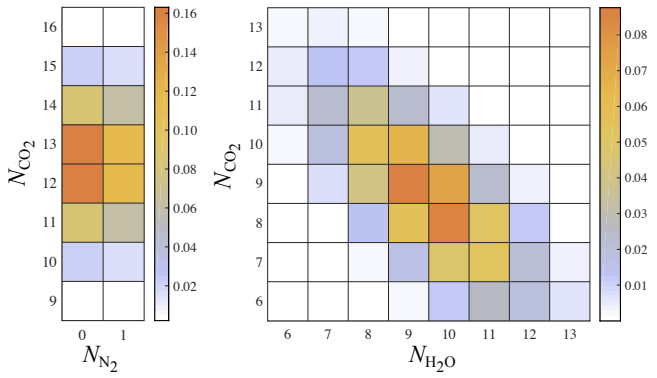

Fig. 3 Probability to observe a configuration with specific numbers of adsorbate molecules per unit cell for the CO_2/N_2 and CO_2/H_2O mixtures.

CO_2/H_2O mixture with partial pressures of 0.15 bar and 1 mbar (about 1% relative humidity) at 313 K, while ignoring N_2 to save computational resources since it binds much weaker. We find that Mg-MOF-74 is highly selective for H_2O over CO_2 ($S_{H_2O} \approx 160$) and that the CO_2 loading is reduced by 3 ± 1 molec/uc (about 25%) compared to the CO_2/N_2 mixture. In comparison, for the ternary mixture of $CO_2/N_2/H_2O$ (171:689:23) Mason *et al.*[40] observed CO_2 and H_2O loadings of 1.1 ± 0.7 molec/uc (i.e., a reduction by a factor of 10 compared to the unary loading) and 31 ± 1, respectively, corresponding to $S_{H_2O} = 210 \pm 150$. For the CO_2/H_2O mixture, IAST performs quite well. The negative slope of unity in the binary loading distribution (see Fig. 3) indicates that H_2O and CO_2 compete for the same strong adsorption sites, and the most likely loadings are those with a total of 18 adsorbate molecules.

In summary, we introduce FPMC simulations for adsorption equilibria that are now feasible for unary and binary mixtures but are, of course, computationally demanding. The ability to describe dative bonding onto strong adsorption sites and the resulting changes in adsorbate–adsorbate interactions (without any parametrization efforts) leads to more accurate predictions for CO_2, N_2, and H_2O adsorption in Mg-MOF-74 than was previously reported with QMDFFs. Combination of the FPMC approach with special MC moves for sampling reactions[42] will allow for fully predictive simulations of reactive multiphase equilibria in nanoporous materials.

This work was supported by the National Science Foundation through Grant CHE-1265849 for the development of the FPMC methodology (E.O.F. & J.I.S.) and by the Department of Energy Office of Basic Energy Sciences, Division of Chemical Sciences, Geosciences and Biosciences under Award DE-FG02-17ER16362 for the simulations of binary mixtures and the analysis. E.O.F. and M.S.S. acknowledge support from University of Minnesota Graduate School Doctoral Dissertation Fellowships. This research used computer resources of the Argonne Leadership Computing Facility, which is a DOE Office of Science User Facility supported under Contract DE-AC02-06CH11357, and at the Minnesota Supercomputing Institute.

Conflicts of interest

There are no conflicts to declare.

Notes and references

1 H. Zhang, J. Nai, L. Yu and X. W. D. Lou, *Joule*, 2017, **1**, 77–107.
2 K. V. Kumar, K. Preuss, M. M. Titirici and F. Rodríguez-Reinoso, *Chem. Rev.*, 2017, **117**, 1796–1825.
3 C. A. Trickett, A. Helal, B. A. Al-Maythalony, Z. H. Yamani, K. E. Cordova and O. M. Yaghi, *Nat. Rev. Mater.*, 2017, **2**, 17045.
4 M. S. Shah, M. Tsapatsis and J. I. Siepmann, *Chem. Rev.*, 2017, **117**, 9755–9803.
5 P. G. Boyd, Y. Lee and B. Smit, *Nat. Rev. Mater.*, 2017, **2**, 17037.
6 Y. G. Chung, D. A. Gómez-Gualdrón, P. Li, K. T. Leperi, P. Deria, H. Zhang, N. A. Vermeulen, F. Stoddart, F. You, J. T. Hupp, O. K. Farha and R. Q. Snurr, *Sci. Adv.*, 2016, **2**, e1600909.
7 J. Yu, L.-H. Xie, J.-R. Li, Y. Ma, J. M. Seminario and P. B. Balbuena, *Chem. Rev.*, 2017, **117**, 9674–9754.
8 A. L. Dzubak, L.-C. Lin, J. Kim, J. a. Swisher, R. Poloni, S. N. Maximoff, B. Smit and L. Gagliardi, *Nat. Chem.*, 2012, **4**, 810–816.
9 A. N. Rudenko, S. Bendt and F. J. Keil, *J. Phys. Chem. C*, 2014, **118**, 16218–16227.
10 E. Haldoupis, J. Borycz, H.-L. Shi, K. D. Vogiatzis, P. Bai, W. L. Queen, L. Gagliardi and J. I. Siepmann, *J. Phys. Chem. C*, 2015, **119**, 16058–16071.
11 R. Mercado, B. Vlaisavljevich, L.-C. Lin, K. Lee, Y. Lee, J. A. Mason, D. J. Xiao, M. I. Gonzalez, M. T. Kapelewski, J. B. Neaton and B. Smit, *J. Phys. Chem. C*, 2016, **120**, 12590–12604.
12 A. Kundu, G. Piccini, K. Sillar and J. Sauer, *J. Am. Chem. Soc.*, 2016, **138**, 14047–14056.
13 J. A. Mason, K. Sumida, Z. R. Herm, R. Krishna and J. R. Long, *Energy Environ. Sci.*, 2011, **4**, 3030–3040.
14 T. G. Glover, G. W. Peterson, B. J. Schindler, D. Britt and O. Yaghi, *Chem. Eng. Sci.*, 2011, **66**, 163–170.
15 D.-A. Yang, H.-Y. Cho, J. Kim, S.-T. Yang and W.-S. Ahn, *Energy Environ. Sci.*, 2012, **5**, 6465–6473.
16 P. M. Schoenecker, C. G. Carson, H. Jasuja, C. J. J. Fleming and K. S. Walton, *Ind. Eng. Chem. Res.*, 2012, **51**, 6513–6519.
17 H. Furukawa, F. Gandara, Y. B. Zhang, J. C. Jiang, W. L. Queen, M. R. Hudson and O. M. Yaghi, *J. Am. Chem. Soc.*, 2014, **136**, 4369–4381.
18 J. Hutter, M. Ianuzzi, F. Schiffmann and J. VandeVondele, *WIREs: Comput. Mol. Sci.*, 2014, **4**, 15–25.
19 M. J. McGrath, J. I. Siepmann, I.-F. W. Kuo, C. J. Mundy, J. VandeVondele, J. Hutter, F. Mohamed and M. Krack, *J. Phys. Chem. A*, 2006, **110**, 640–646.
20 A. Z. Panagiotopoulos, N. Quirke, M. Stapleton and D. J. Tildesley, *Mol. Phys.*, 1988, **63**, 527–545.
21 M. J. McGrath, J. I. Siepmann, I.-F. W. Kuo, C. J. Mundy, J. VandeVondele, J. Hutter, F. Mohamed and M. Krack, *ChemPhysChem*, 2005, **6**, 1894–1901.
22 W. L. Queen, M. R. Hudson, E. D. Bloch, J. A. Mason, M. I. Gonzalez, J. S. Lee, D. Gygi, J. D. Howe, K. Lee, T. A. Darwish, M. James, V. K. Peterson, S. J. Teat, B. Smit, J. B. Neaton, J. R. Long and C. M. Brown, *Chem. Sci.*, 2014, **5**, 4569–4581.
23 D. Fairen-Jimenez, S. A. Moggach, M. T. Wharmby, P. A. Wright, S. Parsons and T. Düren, *J. Am. Chem. Soc.*, 2011, **133**, 8900–8902.
24 F. X. Coudert, A. Boutin, A. H. Fuchs and A. V. Neimark, *J. Phys. Chem. Lett.*, 2013, **4**, 3198–3205.
25 J. Heinen and D. Dubbeldam, *WIREs: Comput. Mol. Sci.*, 2018, **8**, e1363.
26 X. S. Zhao, J. I. Siepmann, Y.-H. Xu, W. Kiang, A. R. Sheth and S. Karaborni, *J. Phys. Chem. B*, 2009, **113**, 5929–5937.
27 S. Duane, A. Kennedy, B. J. Pendleton and D. Roweth, *Phys. Lett. B*, 1987, **195**, 216–222.
28 B. Smit, S. Karaborni and J. I. Siepmann, *J. Chem. Phys.*, 1995, **102**, 2126–2140.
29 L. D. Gelb, *J. Chem. Phys.*, 2003, **118**, 7747–7750.
30 J. P. Perdew, K. Burke and M. Ernzerhof, *Phys. Rev. Lett.*, 1996, **77**, 3865–3868.
31 S. Grimme, J. Antony, S. Ehrlich and H. Krieg, *J. Chem. Phys.*, 2010, **132**, 154104.
32 X. Peng, L.-C. Lin, W. Sun and B. Smit, *AIChE J.*, 2015, **61**, 677–687.
33 B. Vlaisavljevich, J. Huck, Z. Hulvey, K. Lee, J. A. Mason, J. B. Neaton, J. R. Long, C. M. Brown, D. Alfè, A. Michaelides and B. Smit, *J. Phys. Chem. A*, 2017, **121**, 4139–4151.
34 L. Valenzano, B. Civalleri, S. Chavan, G. T. Palomino, C. O. Areán and S. Bordiga, *J. Phys. Chem. C*, 2010, **114**, 11185–11191.
35 K. Tan, S. Zuluaga, Q. Gong, Y. Gao, N. Nijem, J. Li, T. Thonhauser and Y. J. Chabal, *Chem. Mater.*, 2015, **27**, 2203–2217.
36 K. E. Anderson, S. L. Mielke, J. I. Siepmann and D. G. Truhlar, *J. Phys. Chem. A*, 2009, **113**, 2053–2059.
37 O. Talu, *Adv. Colloid Interface Sci.*, 1998, **76-77**, 227 – 269.
38 A. L. Myers and J. M. Prausnitz, *AIChE J.*, 1965, **11**, 121–127.
39 L. Joos, J. A. Swisher and B. Smit, *Langmuir*, 2013, **29**, 15936–15942.
40 J. A. Mason, T. M. McDonald, T.-H. Bae, J. E. Bachman, K. Sumida, J. J. Dutton, S. S. Kaye and J. R. Long, *J. Am. Chem. Soc.*, 2015, **137**, 4787–4803.
41 D. Bahamon, A. Díaz-Márquez, P. Gamallo and L. F. Vega, *Chem. Eng. J.*, 2018, **342**, 458–473.
42 E. O. Fetisov, M. S. Shah, C. Knight, M. Tsapatsis and J. I. Siepmann, *ChemPhysChem*, 2018, **19**, 512–518.

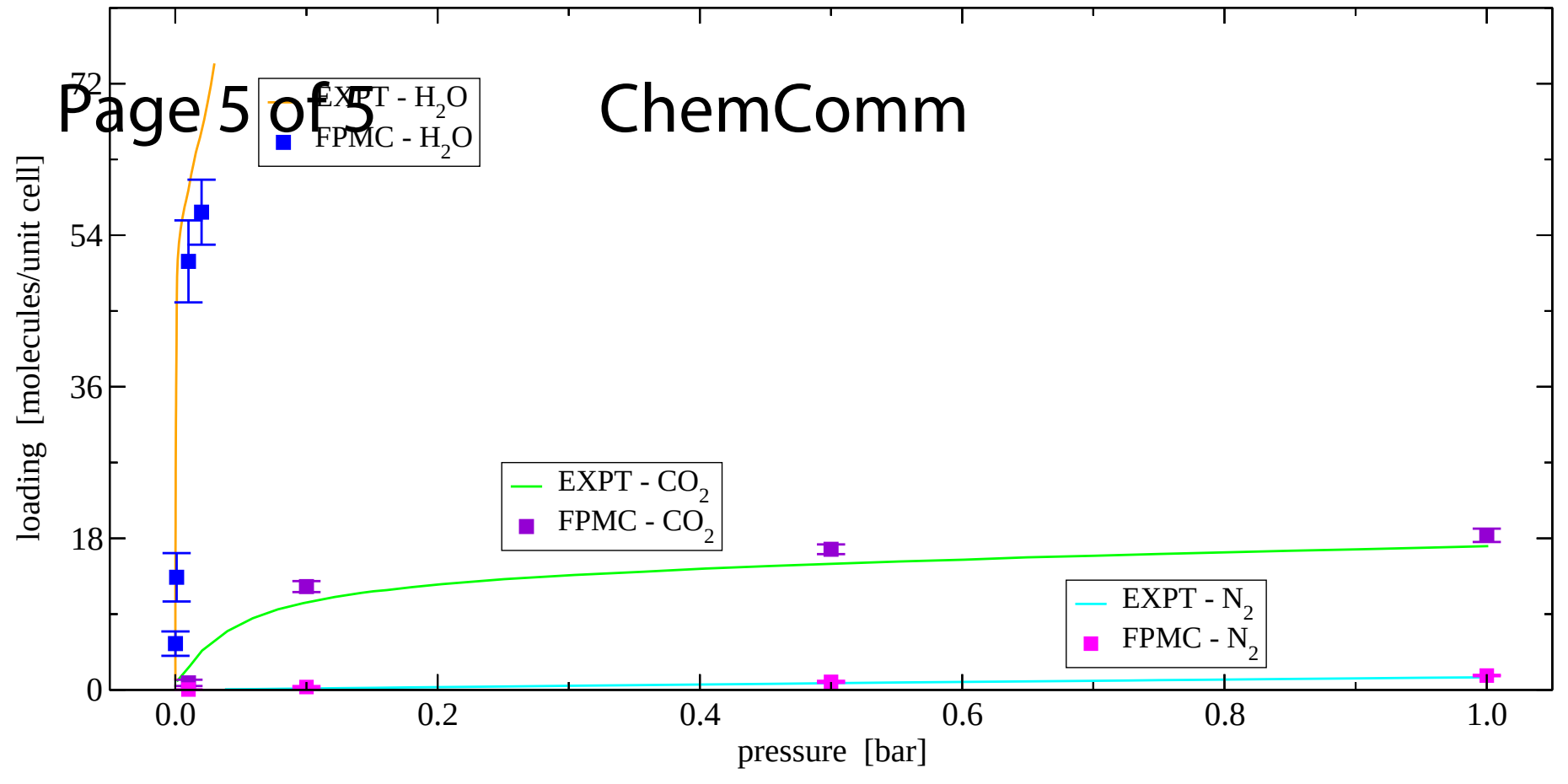
EXPT - H2O
FPMC - H2O
EXPT - CO2
FPMC - CO2
EXPT - N2
FPMC - N2
loading [molecules/unit cell]
pressure [bar]
0
18
36
54
72
0.0
0.2
0.4
0.6
0.8
1.0